m6A reader IGF2BP2 mediates paclitaxel resistance in esophageal squamous cell carcinoma via FOXM1 mRNA stabilization

SHIHENG REN[1-3*], JINGRU WU[1,4*], LENING ZHANG[2], GUANGYI GUAN[4] and WENPENG JIANG[1]

[1]Department of Thoracic Surgery, Shandong Provincial Hospital Affiliated to Shandong First Medical University, Jinan, Shandong 250021, P.R. China; [2]Department of Thoracic Surgery, China-Japan Union Hospital of Jilin University, Changchun, Jilin 130033, P.R. China; [3]Cheeloo College of Medicine, Shandong University, Jinan, Shandong 250012, P.R. China; [4]Shandong First Medical University, Jinan, Shandong 250117, P.R. China

Received December 18, 2024; Accepted August 19, 2025

DOI: 10.3892/or.2025.9002

Abstract. Esophageal squamous cell carcinoma (ESCC) ranks among the primary contributors to cancer-related mortality in China. Resistance to paclitaxel markedly diminishes its therapeutic effectiveness and outcomes. Anaerobic glycolysis is a pivotal mechanism in cancer progression. Insulin-like growth factor 2 mRNA binding protein 2 (IGF2BP2) as a reader of RNA N6-methyladenosine (m6A) modification ensures the stability of RNA at the post-transcriptional level. Nonetheless, the role and mechanism of IGF2BP2 in mediating paclitaxel resistance and anaerobic glycolysis in ESCC remain unclear. The current study selected two ESCC cell lines (KYSE30 and KYSE150). Cell proliferation and clonogenic ability were assessed via functional experiments. Apoptosis was quantified through flow cytometry. The rate of anaerobic glycolysis was determined via glycolysis assays. The stability of Forkhead box M1 (FOXM1) mRNA was assessed through reverse transcription-quantitative polymerase chain reaction following actinomycin D treatment. Protein levels were analyzed through western blotting. Bioinformatics analysis revealed an overexpression of IGF2BP2 in ESCC. Furthermore, IGF2BP2 silencing inhibited cell proliferation and clonogenic activity. RNA and m6A-sequencing results suggested that FOXM1 is critical to IGF2BP2-mediated paclitaxel resistance in ESCC. Additionally, it was discovered that the silencing of IGF2BP2 compromises FOXM1 mRNA stability, reduces anaerobic glycolysis, and diminishes paclitaxel resistance. Finally, FOXM1 overexpression mitigated the effects of IGF2BP2 silencing in ESCC cells. The current findings underscore the significant role of the IGF2BP2-FOXM1 signaling pathway in modulating anaerobic glycolysis and paclitaxel resistance in ESCC, offering insights into future therapeutic approaches to this malignancy.

Correspondence to: Professor Wenpeng Jiang, Department of Thoracic Surgery, Shandong Provincial Hospital Affiliated to Shandong First Medical University, 324 Jing Wu Road, Jinan, Shandong 250021, P.R. China
E-mail: jwp1983@126.com

*Contributed equally

Key words: esophageal squamous cell carcinoma, insulin-like growth factor 2 mRNA binding protein 2, Forkhead box M1, anaerobic glycolysis, paclitaxel resistance

Introduction

Esophageal cancer (EC) represents a major worldwide health challenge, ranking seventh in incidence and sixth in terms of cancer-related mortality (1). There are two main histological variants of EC: Esophageal squamous cell carcinoma (ESCC) and esophageal adenocarcinoma. ESCC is the predominant variant, accounting for 85% of cases worldwide, with Chinese patients representing up to 57% of all instances (2,3). Due to non-specific symptoms in the early stages, a large proportion of ESCC cases are identified at progressive stages (4). Among patients with locally advanced ESCC, ~50% are eligible for R0 resection, while the remaining patients may experience early recurrence post-surgery (5). Neoadjuvant chemotherapy or neoadjuvant chemoradiotherapy in conjunction with transthoracic esophagectomy has become the standard of care, enhancing the R0 resection rate and survival outcomes (6). However, the necessity of radiation therapy in neoadjuvant treatment protocols in China remains a subject of debate (7,8).

Paclitaxel is recognized as an active chemotherapy agent for ESCC, with paclitaxel-based regimens extensively utilized in clinical settings. Nevertheless, response rates for both paclitaxel and cisplatin have been reported to be as low as 33-40% (9). The efficacy of paclitaxel is notably compromised by resistance, which is associated with an increase in postoperative complications and mortality, consequently contributing to chemotherapy failure and unfavorable prognoses (10,11). Therefore, further elucidation of the molecular mechanisms underlying paclitaxel resistance in ESCC is imperative. In this context, intrinsic resistance to paclitaxel in ESCC is attributed to particular genetic, epigenetic and metabolic characteristics (12).

N6-methyladenosine (m6A) represents the most abundant post-transcriptional alteration in eukaryotic messenger RNA (mRNA), serving a crucial function in determining RNA

fate, which encompasses mRNA splicing, export, stability, localization and translation (13). The biological functions of m6A modification undergo dynamic and reversible control by three distinct groups of proteins: RNA m6A methyltransferases (writers), RNA demethylases (erasers) and m6A-binding proteins (readers). The 'readers' specifically identify and engage with the m6A modification, influencing the destiny of target transcripts that exhibit m6A methylation. Among this significant group of readers, insulin-like growth factor 2 mRNA binding proteins (IGF2BPs) function to suppress mRNA degradation and enhance mRNA translation (14). Notably, insulin-like growth factor 2 mRNA binding protein 2 (IGF2BP2) emerges as a prominent member. Studies indicated that IGF2BP2 participates in the metabolism of target mRNAs, encompassing Sirtuin 1 and 5-Hydroxytryptamine Receptor 3A in ESCC (15,16). Nevertheless, the role and mechanisms through which IGF2BP2 contributes to paclitaxel resistance in ESCC remain unclear.

The investigation into the relationship between tumor metabolic characteristics and cancer progression has been gaining increasing attention within the realm of cancer research. Cancer cells exhibit a preference for elevated rates of aerobic glycolysis as their primary source of energy, even when sufficient oxygen is present, and mitochondrial function remains normal (referred to as the Warburg effect). This phenomenon enhances the resistance of cancer cells to apoptotic cell death (17). The aberrantly increased glycolytic rate in tumors is linked to both intrinsic and acquired resistance to standard anticancer therapies (17-19). Therefore, the modulation of tumor metabolism is anticipated to function as a viable therapeutic strategy for multiple cancer types, including ESCC.

In the current study, it was revealed that IGF2BP2 mediated paclitaxel resistance in ESCC and explored the mechanism and identified the IGF2BP2-FOXM1 signaling as a potential biomarker for predicting paclitaxel resistance in ESCC.

Materials and methods

Cell culture. The ESCC cell lines (KYSE30, KYSE150 and KYSE510) utilized in the present study were procured from the Cell Resource Center at the Shanghai Institutes for Biological Sciences, Chinese Academy of Sciences. All cells were cultured in RPMI-1640 medium (Gibco; Thermo Fisher Scientific, Inc.) supplemented with 10% fetal bovine serum and maintained in an incubator at 37˚C with 5% CO_2. The cells were passaged a maximum of 15 times.

Gene expression in ESCC datasets. The gene expression profiles were obtained from The Cancer Genome Atlas (TCGA) (https://portal.gdc.cancer.gov/) and the Gene Expression Omnibus (GEO) (https://www.ncbi.nlm.nih.gov/gds/). RNA sequencing (RNA-seq) data from 82 ESCC tumor samples and 11 adjacent normal tissues were retrieved from the TCGA database. Concurrently, gene expression profiles GSE23400 and GSE75241 were downloaded from the GEO database. Differential gene analysis was conducted on the GSE20347 dataset from the GEO database. To ascertain differentially expressed genes, the criteria |logFC|>1 and adjusted P<0.05 were employed and the differences were visualized using volcano plots.

Plasmids. To generate KYSE30 and KYSE150 cells characterized by FOXM1 overexpression, ESCC cells were transfected with the FOXM1-overexpression plasmid (GV-FOXM1) or negative-control plasmid (GV-Vector) using Lipofectamine™ 3000 (Thermo Fisher Scientific, Inc.) at 37˚C for 6 h, with 2 μg DNA and 5 μg HG-TransGene per well in a 6-well plate, according to the supplier's protocols. The overexpression plasmids utilized in the current study were engineered and constructed by Genomeditech (Shanghai) Co., Ltd. After the culture medium was replaced with fresh complete medium, the efficiency of the FOXM1 overexpression was confirmed. ESCC cells exhibiting FOXM1 overexpression were employed for subsequent experiments 24 h post-medium change.

Cell transfection and lentiviral infection. The IGF2BP2 RNA interference lentiviral vector and the corresponding negative control lentiviral vectors were obtained from Genomeditech (Shanghai) Co., Ltd. The shRNA was synthesized, cloned and inserted into pLKO.1-puro vector. The generation system is the third system. Subsequently, pLKO.1-puro-shRNA plasmid (20 μg), virus packaging plasmids (psPAX2, 15 μg) and envelope plasmids (pMD2.G, 5 μg) were cotransfected into 293T cells (China Center for Type Culture Collection) using Lipofectamine™ 3000 (Thermo Fisher Scientific, Inc.) at 37˚C for 6 h. Then medium was replaced with fresh DMEM (Thermo Fisher Scientific, Inc.) containing 10% FBS and incubated at 37˚C with 5% CO_2. Supernatants were collected at 48 and 72 h post-transfection, filtered through 0.45 μm PVDF membrane and concentrated by ultracentrifugation (100,000 x g). MOI for lentivirus transfection was 10. KYSE30 and KYSE150 cells in the exponential growth phase were seeded in 6-well plates for 24 h. The IGF2BP2 RNA interference and negative control lentivirus were infected into KYSE30 and KYSE150 cells, respectively. Infection was enhanced with 6 μg/ml Polybrene. Following a 24-h infection, the medium was replaced with complete medium, and the cells were cultured. Puromycin (cat. no. P8230; Beijing Solarbio Science & Technology Co., Ltd.) at 5 μg/ml was utilized to select stably transduced cell populations at 72 h post-infection. The subsequent experiment was performed 10 days post-medium change. The sequences of all shRNAs were as follows: shRNA-IGF2BP2-1: 5'-GCCAGAACA CUUCCAAGAUAU-3'; shRNA-IGF2BP2-2: 5'-CAGUUA CUGGAGAUGAUUAAU-3'; shRNA-IGF2BP2-3: 5'-GCU AUCCACAAGGUCAGUAUU-3'; and non-targeting control shRNA: 5'-CCUAAGGUUAAGUCGCCCUCG-3'.

Small interfering RNA (siRNA) of FOXM1 and negative control were obtained from Genomeditech (Shanghai) Co., Ltd. 5 μl siRNA (20 μM) was diluted in 50 μl Opti-MEM (Gibco; Thermo Fisher Scientific, Inc.) and 5 μl of Lipofectamine™ 3000 (Thermo Fisher Scientific, Inc.) was diluted in 250 μl Opti-MEM. After incubating separately for 5 min, the mixtures were combined and further incubated for 20 min. The transfection complex was then added to ESCC cells seeded in 6-well plates for transfection at 37˚C for 6 h. Knockdown efficiency was assessed 24 h after transfection, followed by subsequent experiments. The sequences of all siRNAs were as follows: siRNA-FOXM1-1 sense, 5'-GAAGCGGACCUCAAUGUG AATT-3' and antisense, 5'-UUCACAUUGAGGUCCGCU UCTT-3'; siRNA-FOXM1-2 sense, 5'-GGAGCUCAAGAA

UCUGACUAUTT-3' and antisense, 5'-UAGUCAGAUUCU UGAGCUCCTT-3'; and siRNA-Ctrl sense, 5'-UUCUCCGAA CGUGUCACGUTT-3' and antisense, 5'-ACGUGACACGUU CGGAGAATT-3'.

Actinomycin D treatment assays. ESCC cells were placed in a 6-well plate at $1x10^5$ cells per well and exposed to Actinomycin D (2 μg/ml; Abcam) for 12 h. Subsequently, the measurement of the FOXM1 mRNA level was conducted using a reverse transcription-quantitative polymerase chain reaction (RT-qPCR) assay.

RT-qPCR. According to the manufacturer's instructions, total RNA was extracted from tissues using TRIzol (cat. no. 15596026; Thermo Fisher Scientific, Inc.). The extracted RNA was subsequently converted to cDNA employing the Evo M-MLV RT Premix (cat. no. AG11706; Accurate Biotechnology Co., Ltd.) according to the supplier's instructions. The SYBR® Green Premix Pro Taq HS qPCR kit (cat. no. AG11701; Accurate Biotechnology Co., Ltd.) was used for qPCR, according to the manufacturer's instructions, and the target sequence was amplified using a LightCycler 480II device (Roche Diagnostics). The thermocycling parameters were set as follows: Preincubation for 5 min at 95˚C, followed by 45 cycles of 10 sec at 95˚C, 10 sec at 60˚C, and 10 sec at 72˚C. β-actin was utilized as an internal control, and relative RNA expression was analyzed using the $2^{-\Delta\Delta Cq}$ method (20). The primer sequences were as follows: FOXM1 forward, 5'-GCA GCGACAGGTTAAGGTTGAG-3' and reverse, 5'-AGTGCT GTTGATGGCGAATTGTAT-3'; IGF2BP2 forward, 5'-TCGT CAGAATTATCGGGCACTTC-3' and reverse, 5'-CCTGCT GCTTCACCTGTTGTA-3'; and β-actin forward 5'-TGGCAC CCAGCACAATGAA-3' and reverse, 5'-CTAAGTCATAGT CCGCCTAGAAGCA-3'.

Western blot (WB) analysis. To extract proteins, ESCC cells were lysed in PMSF-containing RIPA buffer solution (cat. no. R0010; Beijing Solarbio Science & Technology Co., Ltd.) and centrifuged at 12,000 x g at 4˚C for 20 min. The protein concentration was determined using the Bicinchoninic acid reagent test kit (Beijing Solarbio Science & Technology Co., Ltd.), according to the manufacturer's instructions. Protein samples (30 μg) were separated by SDS-PAGE on 10% gels (cat. no. PG112; Shanghai EpiZyme Co., Ltd.) and then transferred onto PVDF membranes (cat. no. WGPVDF22; Servicebio Co., Ltd.). Subsequently, the membranes were blocked with high-efficiency western blocking reagent (cat. no. GF1815; Shanghai Genefist Co., Ltd.) for 15 min at room temperature and maintained overnight at 4˚C with the primary antibodies, including anti-IGF2BP2 (1:2,000; cat. no. 11601-1-AP; Proteintech Group, Inc.), anti-FOXM1 (1:2,000; cat. no. 13147-1-AP; Proteintech Group, Inc.) and anti-GAPDH (1:5,000; cat. no. 10494-1-AP; Proteintech Group, Inc.). After rinsing the membrane three times with TBST (cat. no. G2150-1L; Wuhan Servicebio Technology Co., Ltd.), the PVDF membranes were exposed to secondary rabbit antibodies (1:5,000; cat. no. SA00001-2; Proteintech Group, Inc.) for 1 h at ambient temperature. An enhanced chemiluminescence reagent (cat. no. SQ201; Shanghai EpiZyme Co., Ltd.) was employed to detect protein signals. Band intensities were analyzed utilizing ImageJ software (V1.54p; National Institutes of Health), with GAPDH serving as the internal control for normalizing target protein expression.

Cell Counting Kit-8 (CCK-8). ESCC cells in the exponential growth phase from both the control and treated groups were inoculated into a 96-well plate at 3,000 cells per well and maintained for 24, 48, 72 and 96 h. After removing the culture medium, each well was washed with phosphate-buffered saline (PBS), and the CCK-8 reagent (MedChemExpress) was combined with serum-free medium to achieve a concentration of 10%. Subsequently, a volume of 100 μl of the prepared solution was dispensed into each well. Following incubation of the 96-well plate at 37˚C for 1 h, the absorbance of each well was measured at 450 nm.

Colony formation assays. Following the counting of ESCC cells in both the control and treated groups, the cells were placed into 6-well plates at 1,000 cells per well and subsequently cultured in an environment maintained at 37˚C with 5% CO_2. When the count of cells within a single clone colony exceeded 50 or the culture duration surpassed 14 days, the culture medium was aspirated, and the plate underwent PBS washing. Following fixation in 4% paraformaldehyde (Beyotime Institute of Biotechnology) for 30 min, staining was performed using 0.1% crystal violet (Beyotime Institute of Biotechnology) at ambient temperature for 15 min. Colonies were counted utilizing ImageJ software.

5-ethynyl-2'-deoxyuridine (EdU) cell proliferation assays. Exponential growth ESCC cells from both the control and treated groups were inoculated into 96-well plates at 5,000 cells per well and maintained for 24 h. The prepared EdU solution (cat. no. C10310-1; Guangzhou RiboBio Co., Ltd.) was incorporated into the culture medium and incubated for 2 h for EdU labeling. Following the removal of the medium and washing with PBS, 4% paraformaldehyde (Beyotime Institute of Biotechnology) was introduced, and the plates were incubated for 30 min at ambient conditions. Subsequently, glycine solution (MedChemExpress), PBS, and an osmotic agent (Beyotime Institute of Biotechnology) were sequentially added to immobilize the cells. The wells were then subjected to Apollo and DNA staining for 30 min at ambient temperature respectively, with images acquired and analyzed using a fluorescence microscope (magnification, x200).

Flow cytometry. The Annexin V-FITC Cell Apoptosis Detection Kit (cat. no. E-CK-A211; Wuhan Elabscience Biotechnology Co., Ltd.) was employed to evaluate the level of cell apoptosis. ESCC cells underwent trypsin digestion to obtain a single-cell suspension (the density of cells was $5x10^5$/ml). Following a 15-min dual staining procedure with V-FITC and PI in the 200-μl single-cell suspension, the cell specimens were examined via flow cytometry using BD LSRFortessa (BD Biosciences), BD FACSDiva™ software (V7.0; BD Biosciences) and FlowJo software (V10.8.1; FlowJo LLC).

Glycolysis assays. A glycolysis assay was performed utilizing a lactate assay kit (cat. no. 600450; Cayman Chemical Company). Exponentially growing ESCC cells from both the

control and treated groups were inoculated into 96-well plates at 5,000 cells per well. After 24 h, the culture medium was harvested for lactate content assessment. The specimens were examined following the instructions outlined in the reagent kit, the values were noted, and calculations were performed.

RNA-seq. Following transfection of IGF2BP2-knockdown KYSE30 and control cells, the cell samples were collected by scraping and subsequently lysed in TRIzol (cat. no. 15596026; Thermo Fisher Scientific, Inc.) for total RNA extraction. DNase (cat. no. AG12001; Accurate Biotechnology Co., Ltd.) was used to remove genomic DNA contamination. The purity of the sample was determined by NanoPhotometer® (IMPLEN, USA). The concentration and integrity of RNA samples were detected by Agilent 2100 RNA nano 6000 assay kit (cat. no. 5067-1511; Agilent Technology Co., Ltd.). Sequencing libraries were generated using VAHTS Universal V6 RNA-seq Library Prep Kit for Illumina® (cat. no. NR604-01/02; Vazyme Co., Ltd.) following the manufacturer's recommendations. Poly-T magnetic beads were used to isolate mRNA, which was then fragmented. First- and second-strand cDNA were synthesized, purified, and subjected to end repair, adenylation, and adapter ligation. The library was size-selected and enriched by PCR prior to sequencing. The library was quantified using the Bio-RAD CFX 96 fluorescence quantitative PCR instrument with the iQ™ SYBR® Green kit (cat. no. 1708880; Bio-Rad Laboratories, Inc.) to the effective concentration of >10 nM. Sequencing was performed on the Illumina NovaSeq 6000 platform (Illumina, Inc.) with the NovaSeq 6000 S4 Reagent Kit V1.5 (cat. no. 20028312; Illumina, Inc.), generating 150 bp paired-end reads. DESeq2 (V1.44.0) and EdgeR (V3.44.0) were used for Difference analysis (21,22), and the Gene Ontology (GO; http://geneontology.org/) was used for function enrichment analysis.

m6A-qPCR and m6A sequencing (m6A-seq). Total RNA was obtained and purified from ESCC samples with TRIzol (cat. no. 15596026; Thermo Fisher Scientific, Inc.), according to the manufacturer's instructions. Following extraction, RNA was incubated with m6A antibodies utilizing the Magna Methylated RNA Immunoprecipitation m6A Kit (MilliporeSigma) for immunoprecipitation. The concentration of m6A-modified mRNA underwent examination through m6A-qPCR or m6A-seq methodologies (Haplox Biotechnology Co., Ltd.). Primers targeting the negative region of FOXM1 m6A served as negative controls, whereas primers targeting the positive region of FOXM1 m6A were employed as positive controls. For m6A-seq, the enriched m6A RNA underwent reverse transcription to generate cDNA, and the library was prepared per the instructions provided by Illumina's NEBNext Ultra RNA Library Preparation Kit (New England Biolabs, Inc.). High-throughput library sequencing was conducted to acquire sequence information about m6A-modified RNA using the Illumina HiSeq X™ Ten platform (Illumina, Inc.).

Statistical analysis. Statistical analysis was performed utilizing GraphPad Prism 9 (Dotmatics). Data are presented as the mean ± standard deviation (SD). Comparisons among several groups were performed using one-way ANOVA followed by Least Significance Difference test was used for the post hoc test, whereas evaluations between paired groups employed paired Student's t-test. $P<0.05$ was considered to indicate a statistically significant difference.

Results

IGF2BP2 is highly expressed in ESCC. Differential gene analysis was performed utilizing the GSE20347 dataset, which revealed a total of 389 differentially expressed genes, encompassing 226 downregulated and 163 upregulated genes (Fig. 1A). Among these, the 10 most markedly upregulated genes were identified as COL11A1, ZIC1, COL1A2, ECT2, ACKR3, LUM, MFHAS1, FNDC3B, IGF2BP2 and KIF23. Furthermore, a comparison of IGF2BP2 expression levels between ESCC tumor tissues and normal tissue samples from the TCGA database indicated a significant increase in IGF2BP2 expression ($P=0.0014$; Fig. 1B). Data obtained from GSE23400 and GSE75241 confirmed the upregulation of IGF2BP2 in ESCC ($P<0.0001$; Fig. 1C and D). Regarding the ESCC cell lines, RT-qPCR (Fig. 2A) demonstrated a significant upregulation of IGF2BP2 in KYSE30 and KYSE150 relative to HET-1A (the normal esophageal cell line). Consequently, both cell lines were chosen for the following investigations.

IGF2BP2 inhibition decreases anaerobic glycolysis and increases the sensitivity to paclitaxel in ESCC cells. To explore the role of IGF2BP2 in ESCC, alterations in cellular phenotypes were assessed following the inhibition of IGF2BP2 expression in cell lines. Efficient knockdown of IGF2BP2 was achieved using two short-hairpin (sh)RNAs (sh-IGF2BP2-1 and sh-IGF2BP2-2) in both KYSE30 and KYSE150 cells (Fig. 2B). Given that sh-IGF2BP2-1 exhibited the highest efficiency, this sequence was selected for subsequent depletion experiments.

CCK-8 assays were performed to evaluate the influence of IGF2BP2 on the proliferation of ESCC cells. The results demonstrated that IGF2BP2 knockdown resulted in significantly decreased cell proliferation (Fig. 2C). Images obtained from colony formation assays illustrated that silencing IGF2BP2 significantly impaired the formation of colonies of ESCC cells (Fig. 2D). Moreover, EdU assays validated the substantial suppressive effect of IGF2BP2 knockdown on ESCC cell proliferation (Fig. 2E). Additionally, flow cytometry assays indicated that the knockdown of IGF2BP2 markedly enhanced the apoptosis of ESCC cells (Fig. 2F). Notably, it was observed that silencing IGF2BP2 resulted in a reduction of anaerobic glycolysis in KYSE30 and KYSE150 cells (Fig. 2G). Moreover, the depletion of IGF2BP2 significantly enhanced ESCC cell responsiveness to paclitaxel (Fig. 2C-F). Collectively, these findings indicated that IGF2BP2 serves a crucial function in anaerobic glycolysis and resistance to paclitaxel in ESCC cells.

FOXM1 is the m6A modification target of IGF2BP2. To elucidate the mechanism through which IGF2BP2 contributes to paclitaxel resistance in ESCC, RNA-seq was conducted using both IGF2BP2-knockdown KYSE30 and control cells. It was demonstrated that the expression of 1,139 genes was globally modified following IGF2BP2 knockdown, with 424 genes exhibiting upregulation and 715 genes displaying

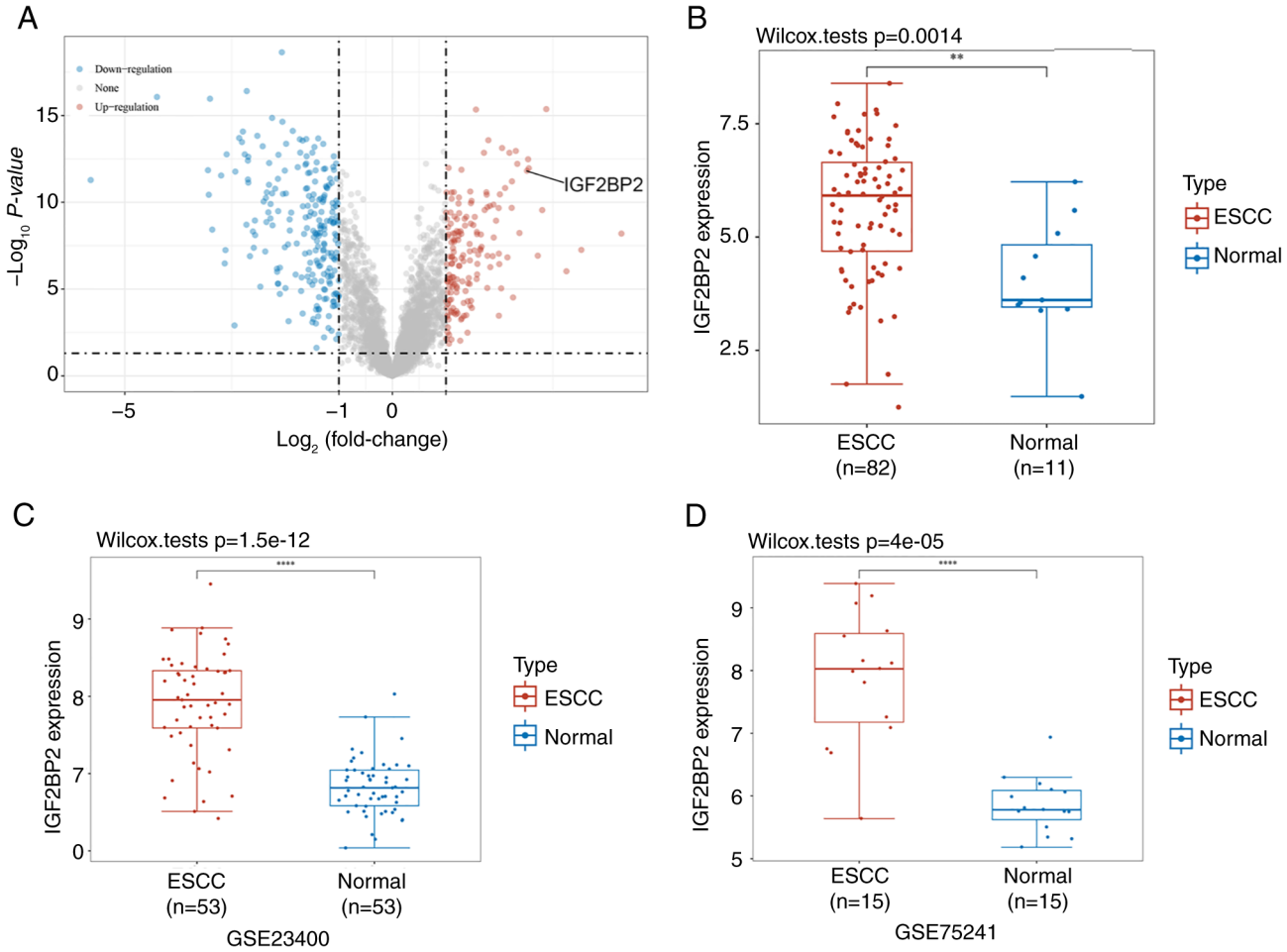

Figure 1. IGF2BP2 as an overexpressed gene is identified in ESCC datasets. (A) Volcano showing GSE20347 differential genes; |LogFC|>1 and P<0.05. (B) Differential expression of IGF2BP2 in The Cancer Genome Atlas ESCC dataset. (C and D) Differential expression of IGF2BP2 in the GSE23400 and GSE75241 datasets. **P<0.01 and ****P<0.0001. IGF2BP2, insulin-like growth factor 2 mRNA binding protein 2; ESCC, esophageal squamous cell carcinoma.

downregulation (Fig. 3A). GO analysis suggested that several pathways, encompassing the MAPK signaling pathway, TGF-β signaling pathway, and protein processing in the endoplasmic reticulum, were markedly enriched (Fig. 3B). These findings collectively highlight the oncogenic role of IGF2BP2 in ESCC.

It is widely acknowledged that IGF2BP2 functions as an m6A reader, capable of recognizing and binding to m6A-methylated transcripts to regulate target genes. Consequently, m6A-seq was conducted in KYSE30 cells, resulting in the identification of 8,104 m6A modification peaks across 3,990 genes. The majority of these m6A modifications were located within the 3'-untranslated regions (3'-UTRs; 43.36%; Fig. 3C). Functional annotation indicated that these mRNAs were associated with several distinct gene clusters, including the regulation of RNA stability and RNA splicing (Fig. 3D). Given that IGF2BP2 has been recognized for its role in maintaining RNA stability (14), the attention was directed towards transcripts that were downregulated following IGF2BP2 knockdown and exhibited the top 100 highest peak m6A modifications. By overlapping the results from RNA-seq and m6A modification analyses, two candidate genes, FOXM1 and SYNCRIP, were identified as meeting the criteria. Among these, FOXM1 mRNA levels declined more markedly upon IGF2BP2 knockdown in ESCC cell lines. Furthermore, emerging evidence suggested that FOXM1 contributes to paclitaxel resistance (23). These findings prompted a shift in focus towards FOXM1, which is considered a critical factor in the mediation of paclitaxel resistance through IGF2BP2 in ESCC (Fig. 3E).

IGF2BP2 sustains the stability of FOXM1 mRNA. To ascertain whether IGF2BP2 modulates FOXM1 expression in ESCC cells, FOXM1 expression was assessed at both transcriptional and translational levels following IGF2BP2 knockdown, utilizing RT-qPCR and WB analysis, respectively. As anticipated, both the RNA expression levels (Fig. 4A) and protein levels (Fig. 4B and C) of FOXM1 exhibited a significant decrease correlating with IGF2BP2 depletion. Given that IGF2BP2 deficiency impaired the levels of FOXM1 mRNA, it was hypothesized that IGF2BP2 may regulate FOXM1 by maintaining the stability of FOXM1 mRNA. Subsequently, 2 g/ml Actinomycin D was administered to treat KYSE30 cells transfected with IGF2BP2-shRNA or control shRNA at various time points. As illustrated in Fig. 4D, a significantly accelerated decay of FOXM1 mRNA was observed in the absence of IGF2BP2 (Fig. 4D), indicating that IGF2BP2 can sustain the stability of FOXM1 mRNA.

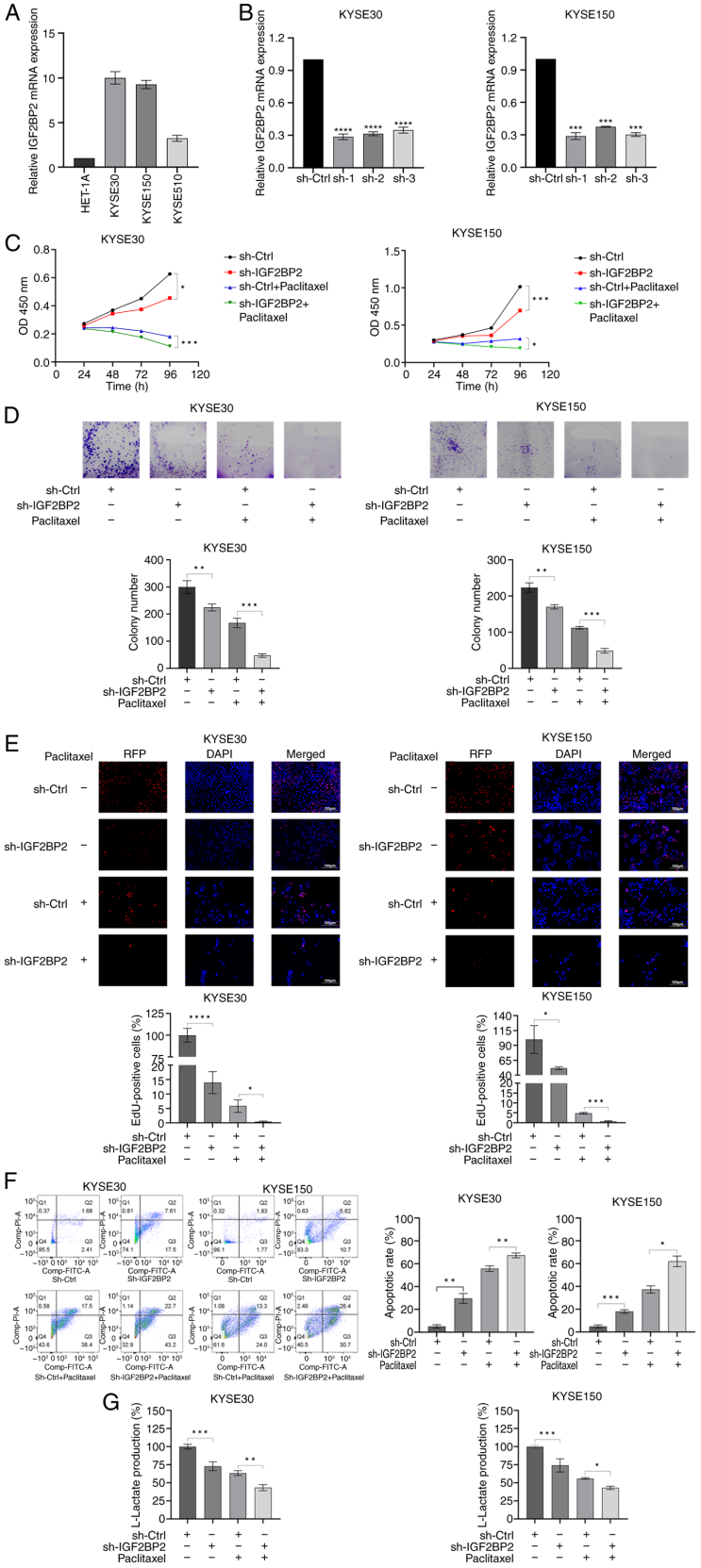

Figure 2. IGF2BP2 plays a vital role in anaerobic glycolysis and resistance to paclitaxel of ESCC cells. (A) IGF2BP2 mRNA expression levels in ESCC cell lines (KYSE30, KYSE150 and KYSE510). (B) Verification of the transfection efficiency of the silencing IGF2BP2 lentivirus detected by reverse transcription-quantitative PCR. (C) Proliferation rates of the control and IGF2BP2 knockdown ESCC cells with and without paclitaxel. (D) Representative images of colony formation showing the proliferation of control and IGF2BP2 knockdown ESCC cells with and without paclitaxel. (E) Representative images showing the proliferation of control and IGF2BP2 knockdown ESCC cells with and without paclitaxel in EdU cell proliferation assay, RFP (red fluorescence imaging channel), DAPI (blue fluorescence imaging channel). (F) Representative images of flow cytometry showing the apoptosis of control and IGF2BP2 knockdown ESCC cells with and without paclitaxel. (G) L-Lactate production level of the control and IGF2BP2 knockdown ESCC cells with and without paclitaxel. *P<0.05, **P<0.01, ***P<0.001 and ****P<0.0001. IGF2BP2, insulin-like growth factor 2 mRNA binding protein 2; ESCC, esophageal squamous cell carcinoma; EdU, 5-ethynyl-2'-deoxyuridine; sh-, short hairpin.

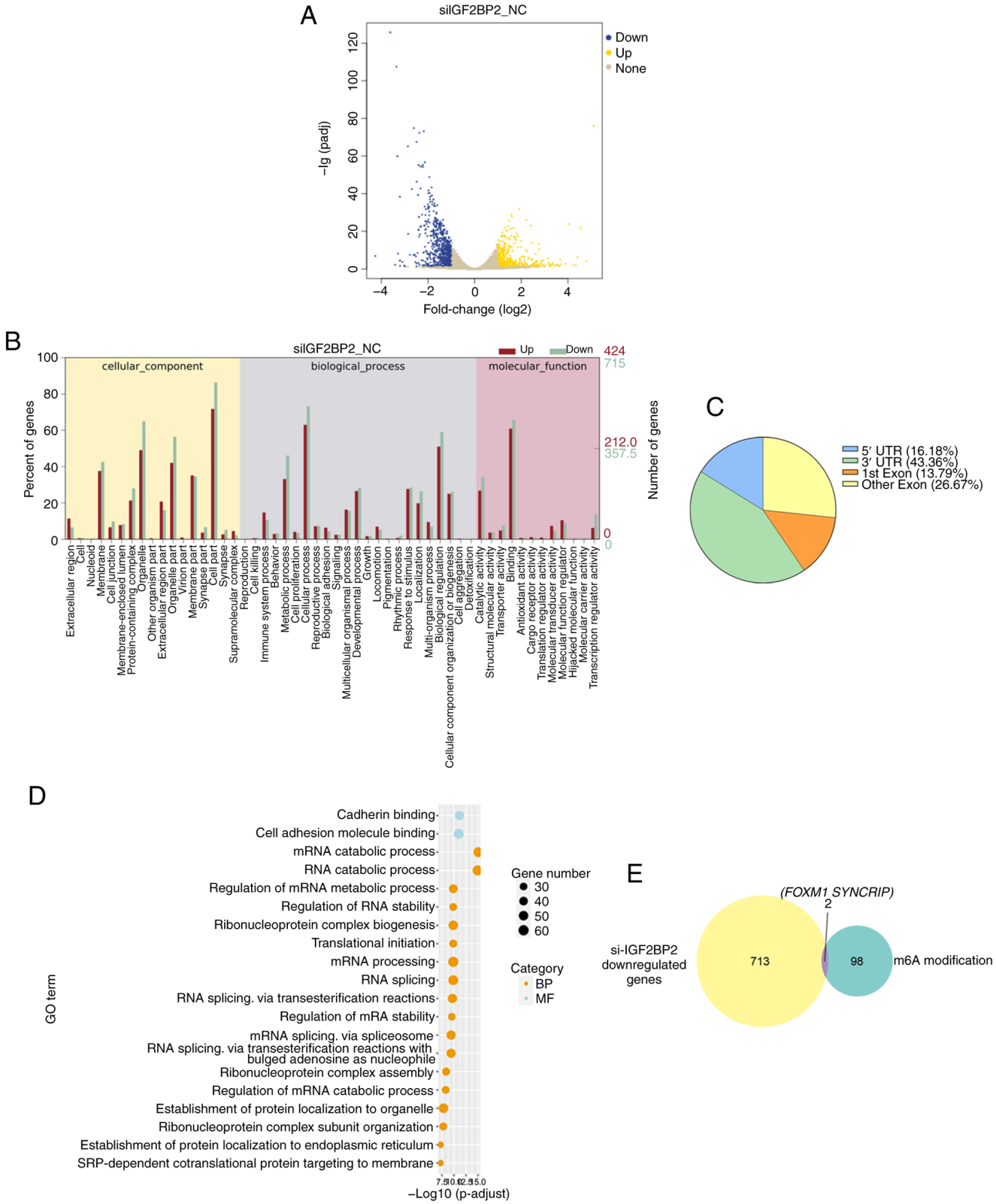

Figure 3. FOXM1 is supposed to be a vital factor in IGF2BP2 mediating the paclitaxel resistance in ESCC. (A) Volcano showing differential genes upon IGF2BP2 knockdown in RNA-sequencing; |LogFC|>1 and P<0.05. (B) GO functional enrichment analysis upon IGF2BP2 knockdown. (C) Distribution of m6A modification peaks on gene elements. (D) GO functional enrichment analysis of m6A-modified genes. (E) Venn diagram showing the intersection of transcripts downregulated by IGF2BP2 knockdown and tagged with the top 100 highest peak m6A modification. FOXM1, Forkhead Box M1; IGF2BP2, insulin-like growth factor 2 mRNA binding protein 2; GO, Gene Ontology; UTR, untranslated region; si-, small interfering; NC, negative control.

FOXM1 serves an oncogenic function in ESCC cells. The oncogenic function of FOXM1 has been documented in ESCC (21-23). To further validate the function of FOXM1 in ESCC, the phenotypes of ESCC cells, encompassing cell growth and proliferation, were examined through gene-loss experiments following FOXM1 depletion (Fig. 5A). Notably,

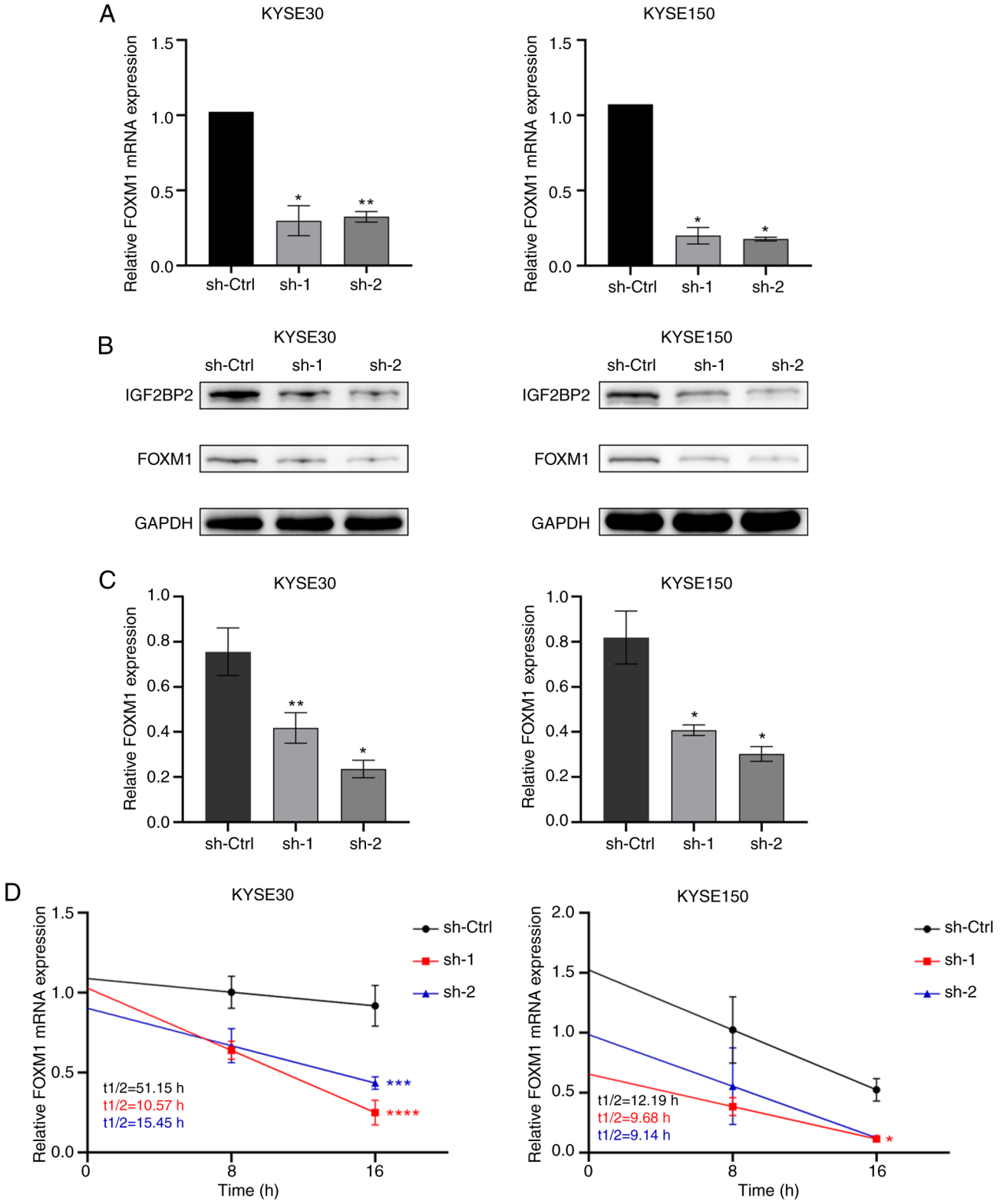

Figure 4. IGF2BP2 sustains the stability of FOXM1 mRNA. (A) Relative FOXM1 mRNA expression in the silencing IGF2BP2 ESCC cells by RT-qPCR. (B) Expression levels of IGF2BP2 and FOXM1 in the control and IGF2BP2 knockdown ESCC cells detected by western blotting. (C) Quantitative analysis of FOXM1 protein abundance with normalization to GAPDH. (D) After treatment with Actinomycin D (2.5 μg/ml) in the control and IGF2BP2 knockdown ESCC cells, the decay rates of mRNA of FOXM1 at certain times were analyzed by RT-qPCR. *P<0.05, **P<0.01, ***P<0.001 and ****P<0.0001. IGF2BP2, insulin-like growth factor 2 mRNA binding protein 2; FOXM1, Forkhead Box M1; ESCC, esophageal squamous cell carcinoma; RT-qPCR, reverse transcription-quantitative PCR; sh-, short hairpin.

a significant reduction in cell growth (Fig. 5B) was observed through the CCK-8 assays, alongside a diminished formation of colonies (Fig. 5C) of the KYSE30 and KYSE150 cells observed in the EdU assays. Consequently, it was hypothesized that FOXM1 facilitates oncogenesis in ESCC cells.

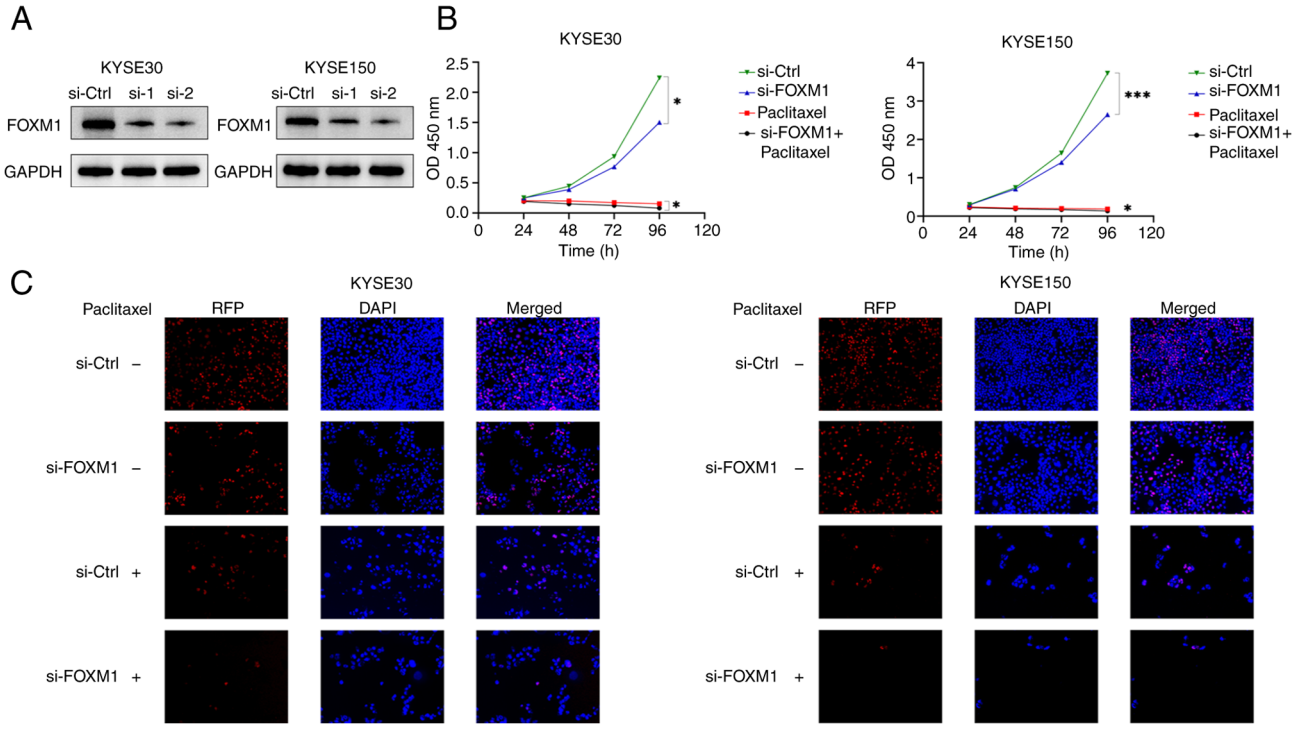

Figure 5. FOXM1 promotes oncogenesis in ESCC cells. (A) Verification of the knockdown efficiency of the siRNA targeting FOXM1 detected by western blotting. (B) Proliferation rates of the control and FOXM1 knockdown ESCC cells with and without paclitaxel. (C) Representative images showing the proliferation of control and FOXM1 knockdown ESCC cells with and without paclitaxel in 5-ethynyl-2'-deoxyuridine cell proliferation assay, RFP (red fluorescence imaging channel), DAPI (blue fluorescence imaging channel). *P<0.05 and ***P<0.001. FOXM1, Forkhead Box M1; ESCC, esophageal squamous cell carcinoma; si-, small interfering.

Ectopic expression of FOXM1 ameliorates the impact of IGF2BP2 deficiency in ESCC cells. To further investigate whether FOXM1 mediates the oncogenic effects of IGF2BP2, FOXM1 expression was upregulated in ESCC cells that were silenced for IGF2BP2. The efficacy of FOXM1 overexpression was validated through WB analysis (Fig. S1A and B). Furthermore, the efficacy of ectopic FOXM1 expression in conjunction with silenced IGF2BP2 was assessed at both transcriptional and translational levels through RT-qPCR and WB analysis, respectively. The results indicated that both RNA expression (Fig. 6A) and protein abundance (Fig. 6B) of ectopically expressed FOXM1 were markedly increased in IGF2BP2-silenced ESCC cells. Subsequently, a series of functional assays were conducted to evaluate ESCC cell activity. CCK-8 assays suggested that the proliferation rate of ESCC cells exhibiting ectopic FOXM1 expression was significantly higher than that of cells lacking ectopic FOXM1, irrespective of the presence of paclitaxel (Fig. 6C). Furthermore, EdU assays illustrated that the reduced cell proliferation activity due to IGF2BP2 depletion was significantly enhanced through ectopic FOXM1 expression (Fig. 6D). The results of colony formation assays corroborated the findings observed in the EdU assays (Fig. 6E). Moreover, flow cytometric analysis revealed that ectopic FOXM1 expression mitigated the apoptosis induced through IGF2BP2 silencing (Fig. 6F). These findings demonstrated that ectopic FOXM1 expression improved cell proliferation, enhanced the formation of colonies and alleviated apoptosis associated with IGF2BP2 deficiency in ESCC cells. Notably, it was observed that the decrease in anaerobic glycolysis resulting from IGF2BP2 silencing in ESCC cells was reversed upon FOXM1 upregulation (Fig. 6G). Therefore, it is proposed that IGF2BP2 promotes anaerobic glycolysis and diminishes sensitivity to paclitaxel in ESCC cells by regulating FOXM1 (Fig. 7).

Discussion

In the current investigation, the overexpression of IGF2BP2 was confirmed, along with its association with paclitaxel resistance and anaerobic glycolysis in ESCC *in vitro*. Mechanistically, it was demonstrated that IGF2BP2 stabilizes FOXM1 mRNA.

Paclitaxel is extensively utilized in combination chemotherapy for ESCC. However, tumor resistance to paclitaxel frequently results in treatment failure, prompting considerable attention towards underlying the mechanisms. Wu *et al* (12) conducted single-cell RNA-seq experiments to elucidate the heterogeneity of gene expression in paclitaxel-resistant ESCC cells, which may contribute to the observed resistance. The findings were validated through drug toxicity assays, colony formation assays and rodent xenograft model experiments. It was concluded that intrinsic paclitaxel resistance exists in KYSE30 ESCC cells, with potential association with KRT19 expression. In the current study, KYSE30 ESCC cells were similarly selected to focus on the role of the m6A reader IGF2BP2 in paclitaxel resistance within ESCC. RNA m6A modification has been reported to mediate paclitaxel resistance in various malignancies. Liu *et al* (27) demonstrated that lncRNA RFPL1S-202 was capable of boosting paclitaxel cytotoxicity in ovarian cancer by physically interacting with

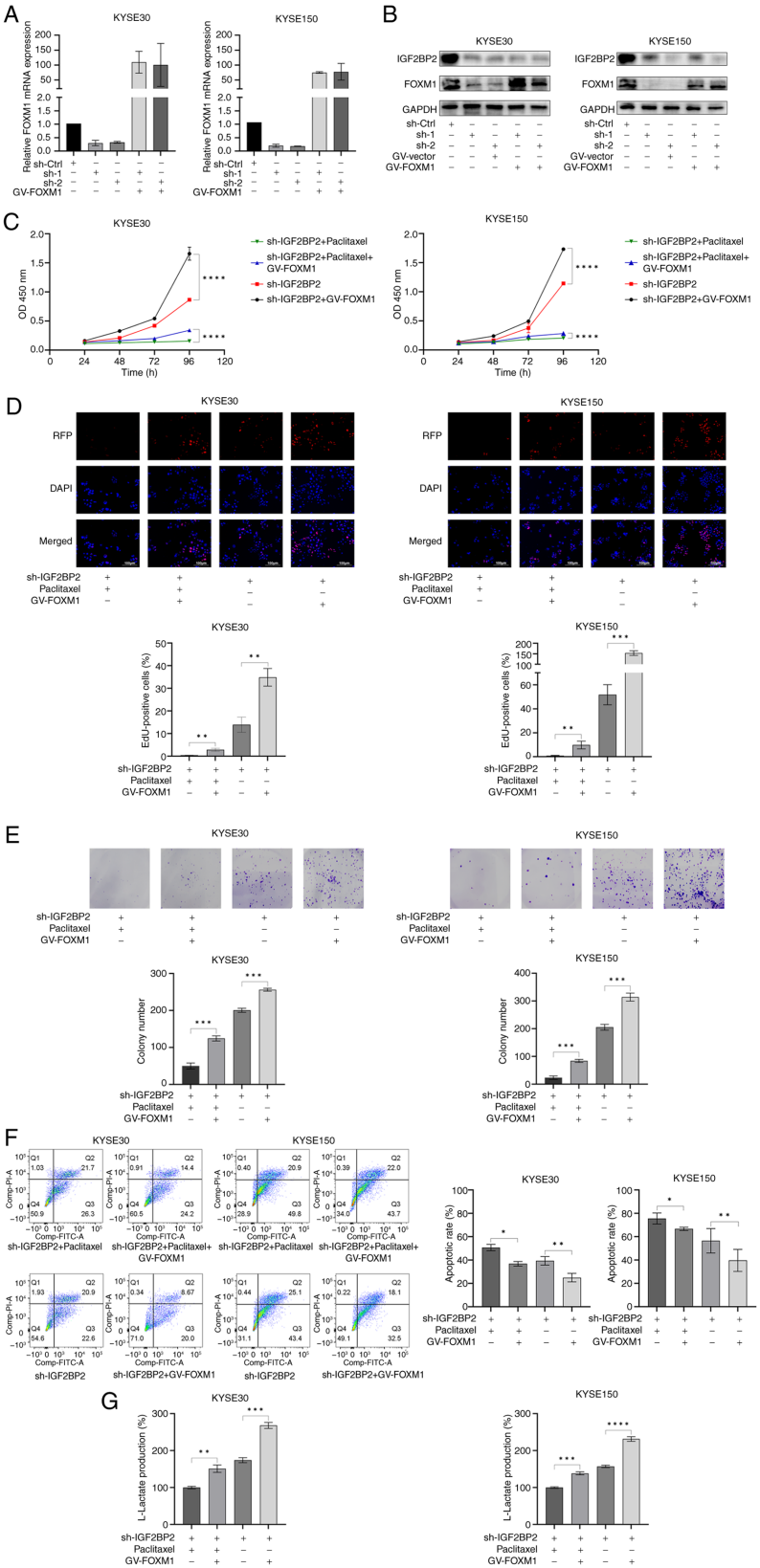

Figure 6. FOXM1 overexpression ameliorates effect of IGF2BP2 deficiency in ESCC cells. (A) Relative FOXM1 mRNA expression in the IGF2BP2 knockdown and FOXM1 overexpression ESCC cells by reverse transcription-quantitative PCR. (B) Expression levels of IGF2BP2 and FOXM1 in the IGF2BP2 knockdown and FOXM1 overexpression ESCC cells detected by western blotting. (C) Proliferation rates of the IGF2BP2 knockdown and FOXM1 overexpression ESCC cells with and without paclitaxel. (D) Representative images showing the proliferation of IGF2BP2 knockdown and FOXM1 overexpression ESCC cells with and without paclitaxel in 5-ethynyl-2'-deoxyuridine cell proliferation assay, RFP (red fluorescence imaging channel), DAPI (blue fluorescence imaging channel). (E) Representative images of colony formation showing the proliferation of the IGF2BP2 knockdown and FOXM1 overexpression ESCC cells with and without paclitaxel. (F) Representative images of flow cytometry showing the apoptosis of IGF2BP2 knockdown and FOXM1 overexpression ESCC cells with and without paclitaxel. (G) L-Lactate production level of the control and IGF2BP2 knockdown ESCC cells with and without paclitaxel. *P<0.05, **P<0.01, ***P<0.001 and ****P<0.0001. FOXM1, Forkhead Box M1; IGF2BP2, insulin-like growth factor 2 mRNA binding protein 2; ESCC, esophageal squamous cell carcinoma.

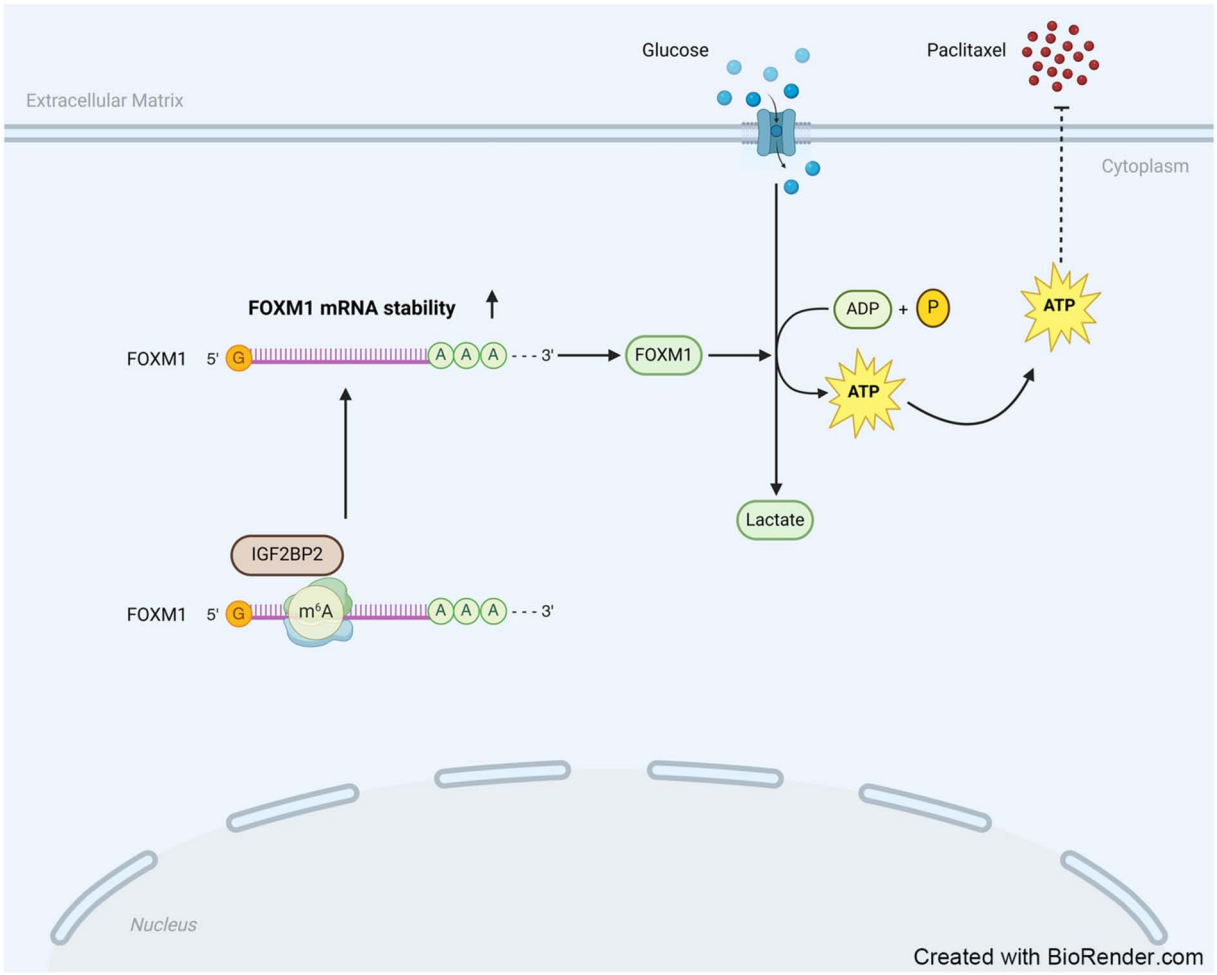

Figure 7. IGF2BP2-mediated FOXM1 promotes anaerobic glycolysis and inhibits sensitivity to paclitaxel of esophageal squamous cell carcinoma cells. IGF2BP2, insulin-like growth factor 2 mRNA binding protein 2; FOXM1, Forkhead Box M1.

DEAD-Box Helicase 3 X-linked (DDX3X) protein, thereby increasing the m6A modification of IFNB1 to reduce the expression of IFN-inducible genes. Additionally, Xie *et al* (28) reported that LINC02489 with m6A modification linked to PKNOX2 via the PTEN/mTOR axis, thereby enhancing the sensitivity of ovarian cancer to paclitaxel and reducing the migration and invasion of chemotherapy-resistant ovarian cancer cells.

A recent study reported that m6A reader IGF2BP2 is upregulated in ESCC tissues in comparison with normal esophageal mucosa. Li *et al* (29) demonstrated a significant upregulation of IGF2BP2 in ESCC tissues through epi-transcriptomics. Additionally, Wang *et al* (30) suggested that IGF2BP2 exhibits elevated expression in ESCC than those in normal esophageal tissues, with its overexpression being closely linked to lymph node metastasis. In the present study, the upregulation of IGF2BP2 in ESCC was confirmed, consistent with previous findings (26-28).

Furthermore, it was demonstrated for the first time that IGF2BP2 expression is positively linked to paclitaxel resistance in ESCC. The current study serves as a valuable supplement to the understanding of m6A modification in the regulation of paclitaxel resistance across various malignancies. One of the hallmarks of cancer is the observation that, even in the presence of normal oxygen concentrations, cancer cells predominantly generate energy through glycolysis at elevated rates, a phenomenon referred to as the Warburg effect. In addition to its tumor-promoting properties, aerobic glycolysis is capable of enhancing drug resistance in cancer cells by creating a supportive microenvironment (32). Consequently, this may present a novel clinical approach, suggesting that the inhibition of glycolysis could partially reverse chemotherapy resistance.

Enhanced sensitivity of KYSE150 ESCC cells to cisplatin, both *in vitro* and *in vivo*, was reported to be associated with inhibited glycolysis, as evidenced by reduced glucose consumption and diminished lactate production. This observation suggests that enhancing the sensitivity of ESCC to cisplatin could be achieved through the reduction of glycolysis (33). Wu *et al* (34) demonstrated that disrupted glycolysis was positively correlated with paclitaxel resistance in epithelial ovarian cancer. In the present study, it was revealed for the first time, to the best of our knowledge, that the inhibition of IGF2BP2 markedly reversed paclitaxel resistance while concurrently decreasing anaerobic glycolysis in ESCC. Further study will be implemented to investigate whether IGF2BP2 mediates paclitaxel resistance in ESCC by modulating glycolytic pathways.

As an m6A reader, the biological function of IGF2BP2 is contingent upon its interaction with m6A-modified RNA. In the present study, m6A modifications in ESCC were systematically screened, revealing a prevalence of such modifications in the UTRs of mRNAs, aligning with previous findings (35). Concurrently, transcriptional analysis following IGF2BP2 knockdown in ESCC cells indicated that the majority of transcripts exhibiting m6A modification were downregulated, suggesting that IGF2BP2 maintains mRNA stability in an m6A-dependent manner within ESCC. Among these genes, it was confirmed that FOXM1 serves as a direct target of IGF2BP2 in ESCC. A previous study indicated that the Akt/FOXM1 signaling cascade inhibits paclitaxel-induced cell death in ESCC (23). In the present investigation, it was established that FOXM1 is modulated by IGF2BP2 at both transcriptional and translational levels in ESCC. Further experiments demonstrated that FOXM1 represents a pivotal factor through which IGF2BP2 mediates paclitaxel resistance and aberrant anaerobic glycolysis in ESCC. The results showed that the FOXM1 transcript is m6A-modified and its expression decreases upon IGF2BP2 knockdown, indicating that IGF2BP2 regulates FOXM1 expression in an m6A-dependent manner.

While the current findings yielded several significant conclusions, certain limitations persist. The mechanism by which IGF2BP2 regulates FOXM1 in an m6A-dependent manner remains to be experimentally substantiated due to the complexity of the associated experiments. IGF2BP2 comprises six canonical RNA-binding domains, encompassing two RNA recognition motifs and four K homology domains. It has been established that the KH3-4 di-domains are critical for IGF2BP2 to bind to m6A-modified mRNAs and modulate the expression of target genes. In forthcoming research, basic experiments will be undertaken to elucidate the mechanism by which IGF2BP2 regulates FOXM1 through the creation of an IGF2BP2 mutant featuring alterations in the KH domains, alongside an assessment of the interaction between IGF2BP2 and FOXM1 mRNA.

In conclusion, the present study demonstrated the significant role of IGF2BP2-FOXM1 signaling in modulating paclitaxel resistance in ESCC. The insights and conclusions presented may offer novel directions for the effective treatment of ESCC.

Acknowledgements

Not applicable.

Funding

The present study was supported by the Natural Science Foundation of Shandong (grant no. ZR2021MH155).

Availability of data and materials

The data generated in the present study may be requested from the corresponding author. The data generated in the present study may be found in the Figshare under accession number 10.6084/m9.figshare.29312819.v2 or at the following URL: (https://doi.org/10.6084/m9.figshare.29312819.v2).

Authors' contributions

SR and WJ conceived and designed the study. SR and JW performed the experiments. JW conducted statistical analysis using GraphPad Prism. GG performed bioinformatics analysis. LZ assisted in experiments, contributed to manuscript editing based on reviewers' comments and revised figures. WJ secured funding, supervised the project and provided critical revision of the manuscript. All authors contributed to the writing and revision of the article. All authors read and approved the final version of the manuscript. SR and WJ confirm the authenticity of all the raw data.

Ethics approval and consent to participate

Not applicable.

Patient consent for publication

Not applicable.

Competing interests

The authors declare that they have no competing interests.

References

1. Sung H, Ferlay J, Siegel RL, Laversanne M, Soerjomataram I, Jemal A and Bray F: Global Cancer statistics 2020: GLOBOCAN estimates of incidence and mortality worldwide for 36 cancers in 185 countries. CA Cancer J Clin 71: 209-249, 2021.
2. Abnet CC, Arnold M and Wei WQ: Epidemiology of esophageal squamous cell carcinoma. Gastroenterology 154: 360-373, 2018.
3. Morgan E, Soerjomataram I, Rumgay H, Coleman HG, Thrift AP, Vignat J, Laversanne M, Ferlay J and Arnold M: The Global landscape of esophageal squamous cell carcinoma and esophageal adenocarcinoma incidence and mortality in 2020 and projections to 2040: New estimates from GLOBOCAN 2020. Gastroenterology 163: 649-658.e2, 2022.
4. An L, Zheng R, Zeng H, Zhang S, Chen R, Wang S, Sun K, Li L, Wei W and He J: The survival of esophageal cancer by subtype in China with comparison to the United States. Int J Cancer 152: 151-161, 2023.
5. Rustgi AK and El-Serag HB: Esophageal carcinoma. N Engl J Med 371: 2499-2509, 2014.
6. Leng XF, Daiko H, Han YT and Mao YS: Optimal preoperative neoadjuvant therapy for resectable locally advanced esophageal squamous cell carcinoma. Ann N Y Acad Sci 1482: 213-224, 2020.
7. Zhu H, Ma X, Ye T, Wang H, Wang Z, Liu Q and Zhao K: Esophageal cancer in China: Practice and research in the new era. Int J Cancer 152: 1741-1751, 2023.
8. Yang H, Liu H, Chen Y, Zhu C, Fang W, Yu Z, Mao W, Xiang J, Han Y, Chen Z, *et al*: Neoadjuvant Chemoradiotherapy followed by surgery versus surgery alone for locally advanced squamous cell carcinoma of the esophagus (NEOCRTEC5010): A phase III multicenter, randomized, open-label clinical trial. J Clin Oncol 36: 2796-2803, 2018.
9. Kotecki N, Hiret S, Etienne PL, Penel N, Tresch E, François E, Galais MP, Ben Abdelghani M, Michel P, Dahan L, *et al*: First-line chemotherapy for metastatic esophageal squamous cell carcinoma: Clinico-biological predictors of disease control. Oncology 90: 88-96, 2016.
10. Mariette C, Dahan L, Mornex F, Maillard E, Thomas PA, Meunier B, Boige V, Pezet D, Robb WB, Le Brun-Ly V, *et al*: Surgery alone versus chemoradiotherapy followed by surgery for stage I and II esophageal cancer: Final analysis of randomized controlled phase III trial FFCD 9901. J Clin Oncol 32: 2416-2422, 2014.

11. Chan KKW, Saluja R, Delos Santos K, Lien K, Shah K, Cramarossa G, Zhu X and Wong RKS: Neoadjuvant treatments for locally advanced, resectable esophageal cancer: A network meta-analysis. Int J Cancer 143: 430-437, 2018.
12. Wu H, Chen S, Yu J, Li Y, Zhang XY, Yang L, Zhang H, Hou Q, Jiang M, Brunicardi FC, *et al*: Single-cell Transcriptome analyses reveal molecular signals to intrinsic and acquired paclitaxel resistance in esophageal squamous cancer cells. Cancer Lett 420: 156-167, 2018.
13. Meyer KD and Jaffrey SR: The dynamic epitranscriptome: N6-methyladenosine and gene expression control. Nat Rev Mol Cell Biol 15: 313-326, 2014.
14. Huang H, Weng H, Sun W, Qin X, Shi H, Wu H, Zhao BS, Mesquita A, Liu C, Yuan CL, *et al*: Recognition of RNA N^6-methyladenosine by IGF2BP proteins enhances mRNA stability and translation. Nat Cell Biol 20: 285-295, 2018.
15. Yang Z, Wan J, Ma L, Li Z, Yang R, Yang H, Li J, Zhou F and Ming L: Long non-coding RNA HOXC-AS1 exerts its oncogenic effects in esophageal squamous cell carcinoma by interaction with IGF2BP2 to stabilize SIRT1 expression. J Clin Lab Anal 37: e24801, 2023.
16. Huang GW, Chen QQ, Ma CC, Xie LH and Gu J: Linc01305 promotes metastasis and proliferation of esophageal squamous cell carcinoma through interacting with IGF2BP2 and IGF2BP3 to stabilize HTR3A mRNA. Int J Biochem Cell Biol 136: 106015, 2021.
17. Liberti MV and Locasale JW: The warburg effect: How does it benefit cancer cells? Trends Biochem Sci 41: 211-218, 2016.
18. Haque MM and Desai KV: Pathways to endocrine therapy resistance in breast cancer. Front Endocrinol (Lausanne) 10: 573, 2019.
19. Ma L and Zong X: Metabolic symbiosis in Chemoresistance: Refocusing the role of aerobic glycolysis. Front Oncol 10: 5, 2020.
20. Livak KJ and Schmittgen TD: Analysis of relative gene expression data using real-time quantitative PCR and the 2(-Delta Delta C(T)) method. Methods 25: 402-408, 2001.
21. Love MI, Huber W and Anders S: Moderated estimation of fold change and dispersion for RNA-seq data with DESeq2. Genome Biol 15: 550, 2014.
22. Robinson MD, McCarthy DJ and Smyth GK: edgeR: A Bioconductor package for differential expression analysis of digital gene expression data. Bioinformatics 26: 139-140, 2010.
23. Meng RY, Jin H, Nguyen TV, Chai OH, Park BH and Kim SM: Ursolic acid accelerates paclitaxel-induced cell death in esophageal cancer cells by suppressing Akt/FOXM1 signaling cascade. Int J Mol Sci 22: 11486, 2021.
24. Hu C, Liu T, Han C, Xuan Y, Jiang D, Sun Y, Zhang X, Zhang W, Xu Y, Liu Y, *et al*: HPV E6/E7 promotes aerobic glycolysis in cervical cancer by regulating IGF2BP2 to stabilize m^6A-MYC expression. Int J Biol Sci 18: 507-521, 2022.
25. Pu J, Wang J, Qin Z, Wang A, Zhang Y, Wu X, Wu Y, Li W, Xu Z, Lu Y, *et al*: IGF2BP2 promotes liver cancer growth through an m6A-FEN1-dependent mechanism. Front Oncol 10: 578816, 2020.
26. Wang Y, Lu JH, Wu QN, Jin Y, Wang DS, Chen YX, Liu J, Luo XJ, Meng Q, Pu HY, *et al*: LncRNA LINRIS stabilizes IGF2BP2 and promotes the aerobic glycolysis in colorectal cancer. Mol Cancer 18: 174, 2019.
27. Liu S, Chen X, Huang K, Xiong X, Shi Y, Wang X, Pan X, Cong Y, Sun Y, Ge L, *et al*: Long noncoding RNA RFPL1S-202 inhibits ovarian cancer progression by downregulating the IFN-β/STAT1 signaling. Exp Cell Res 422: 113438, 2023.
28. Xie Y, Wang L, Luo Y, Chen H, Yang Y, Shen Q and Cao G: LINC02489 with m6a modification increase paclitaxel sensitivity by inhibiting migration and invasion of ovarian cancer cells. Biotechnol Genet Eng Rev 39: 1128-1142, 2023.
29. Li Y, Xiao Z, Wang Y, Zhang D and Chen Z: The m^6A reader IGF2BP2 promotes esophageal cell carcinoma progression by enhancing EIF4A1 translation. Cancer Cell Int 24: 162, 2024.
30. Wang C, Zhou M, Zhu P, Ju C, Sheng J, Du D, Wan J, Yin H, Xing Y, Li H, *et al*: IGF2BP2-induced circRUNX1 facilitates the growth and metastasis of esophageal squamous cell carcinoma through miR-449b-5p/FOXP3 axis. J Exp Clin Cancer Res 41: 347, 2022.
31. Xiao Y, Tang J, Yang D, Zhang B, Wu J, Wu Z, Liao Q, Wang H, Wang W and Su M: Long noncoding RNA LIPH-4 promotes esophageal squamous cell carcinoma progression by regulating the miR-216b/IGF2BP2 axis. Biomark Res 10: 60, 2022.
32. Bhattacharya B, Mohd Omar MF and Soong R: The Warburg effect and drug resistance. Br J Pharmacol 173: 970-979, 2016.
33. Fang J, Ma Y, Li Y, Li J, Zhang X, Han X, Ma S and Guan F: CCT4 knockdown enhances the sensitivity of cisplatin by inhibiting glycolysis in human esophageal squamous cell carcinomas. Mol Carcinog 61: 1043-1055, 2022.
34. Wu X, Qiu L, Feng H, Zhang H, Yu H, Du Y, Wu H, Zhu S, Ruan Y and Jiang H: KHDRBS3 promotes paclitaxel resistance and induces glycolysis through modulated MIR17HG/CLDN6 signaling in epithelial ovarian cancer. Life Sci 293: 120328, 2022.
35. Zaccara S, Ries RJ and Jaffrey SR: Reading, writing and erasing mRNA methylation. Nat Rev Mol Cell Biol 20: 608-624, 2019.